System-on-Chip Design for Ultrasonic Target Detection Using Split-Spectrum Processing and Neural Networks

Jafar Saniie, *Fellow, IEEE*, Erdal Oruklu, *Senior Member, IEEE*, and Sungjoon Yoon

Abstract—Ultrasonic detection and characterization of targets concealed by scattering noise is remarkably challenging. In this study, a neural network (NN) coupled to split-spectrum processing (SSP) is examined for target echo visibility enhancement using experimental measurements with input signal-to-noise ratio around 0 dB. The SSP-NN target detection system is trainable and consequently is capable of improving the target-to-clutter ratio by an average of 40 dB. The proposed system is exceptionally robust and outperforms the conventional techniques such as minimum, median, average, geometric mean, and polarity threshold detectors. For real-time imaging applications, a field-programmable gate array (FPGA)-based hardware platform is designed for system-on-chip (SoC) realization of the SSP-NN target detection system. This platform is a hardware/software co-design system using parallel and pipelined multiplications and additions for high-speed operation and high computational throughput.

I. Introduction

ULTRASONIC imaging has a wide range of applications, from nondestructive evaluation of materials to medical imaging and diagnosis. In ultrasonic imaging, scattering echoes resulting from the microstructure of materials consisting of a large number of complex and randomly distributed scatterers often mask the target echo to an extent that misdetection becomes the norm rather than an exception. Scattering noise, known as clutter, is a common problem which affects a wide range of detection and imaging applications including radar, optics, and sonar. When scatterers are stationary, as is the case in ultrasonic imaging, the clutter suppression cannot be achieved by signal averaging. Furthermore, clutter and target echoes span the same frequency range and signal filtering is also ineffective. Nevertheless, it is feasible to decorrelate clutter and improve target visibility by shifting the frequency band of the transmitter/receiver (using multiple channels) and to obtain a set of frequency-diverse signals. Clutter decorrelation by frequency diversity (also known as frequency agility when frequency shifts from pulse to pulse using a single channel) for radar target detection dates back to the 1960s [1]–[5]. In the 1980s and 1990s, frequency-diverse detection was explored for both ultrasonic imaging and radar target detection applications [6]–[11].

These investigations led to the development of the theory of signal sub-band decomposition followed by the Bayesian [12] and order statistics [8], [13] post-detection processors.

For ultrasonic target detection and classification applications, the presence of high scattering noise poses a significant and challenging problem. This paper presents techniques based on frequency-diverse ultrasonic imaging which induces significant statistical variation in ultrasonic scattering noise or speckles resulting from the microstructure of objects under examination. In particular, frequency-diverse imaging is achieved through split-spectrum processing (SSP), which performs sub-band signal decomposition. Post-processing methods including order statistics (OS) and neural networks (NNs) are utilized to improve target echo visibility in the presence of clutter that is significantly intense compared with the target echo. The adaptive learning capability of NNs results in considerably more robust detection performance compared with conventional techniques [8], [12], [13].

In this paper, experimental results are presented for evaluating the significance of target-to-clutter ratio (TCR) improvement with the proposed SSP-NN technique. Furthermore, a field-programmable gate array (FPGA)-based hardware platform is designed for system-on-chip (SoC) realization of a real-time ultrasonic imaging system. In particular, embedded hardware/software co-design has been developed to make this multifaceted computing and detection system realizable.

II. Ultrasonic Signal Sub-Band Decomposition

A well-established technique for obtaining frequency diverse information is signal sub-band decomposition, also known as split-spectrum processing (SSP) [6]. As shown in Fig. 1, the SSP method has five major components. The front-end component is the data acquisition subsystem. The second module is the fast Fourier transform (FFT) component, which computes the frequency spectrum of the received echo signal. The third component includes several sub-band filters, which split the spectrum into different frequency bands as shown in Fig. 2. The next computation step generates inverse FFTs corresponding to the time-domain signal of each individual frequency band. As the final processing step, the signals from each individual frequency band are first normalized and then passed into a post-processor. This post-processor can employ different techniques such as averaging, minimization, order statistic
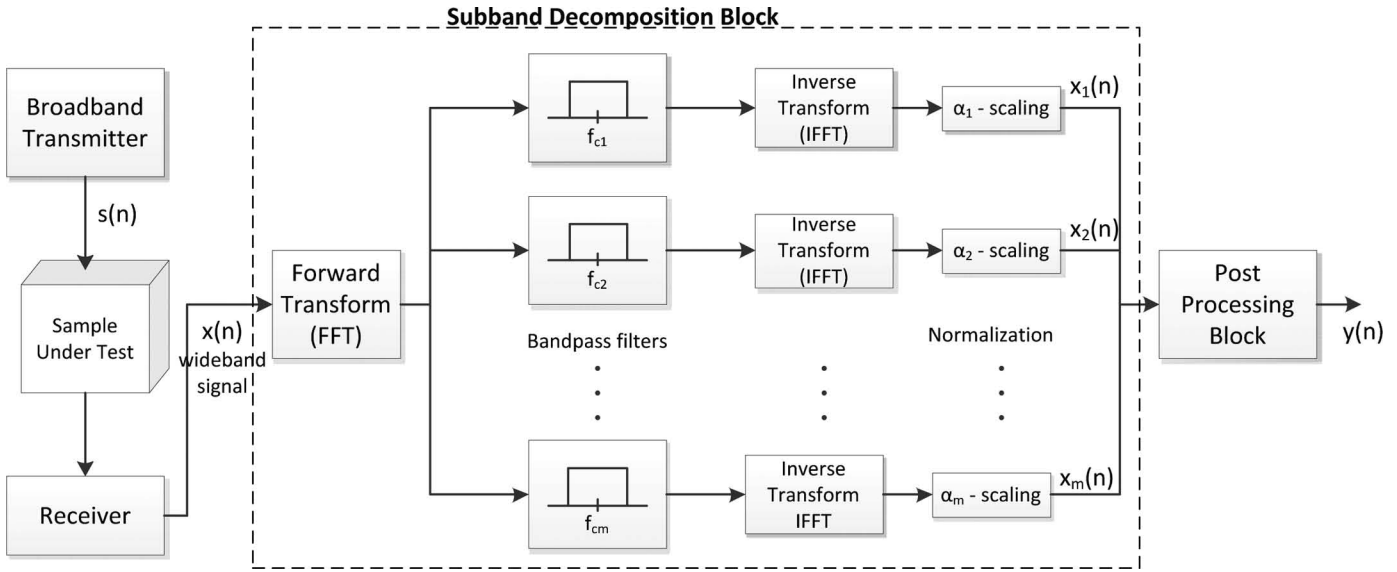
Fig. 1. Target echo visibility enhancement based on split-spectrum processing.

filters, or Bayesian classifiers [9], [10], [12], [14] to differentiate target echoes from clutter.

The performance of SSP is profoundly influenced by the number of band-pass filtering channels (or observations) across the signal spectrum, and the correlation between the observations and statistical information in each channel. Increasing the number of channels corresponding to the output of band-pass filters, increases the likelihood of detecting target echoes against the undesirable microstructure scattering noise. However, there exists only a limited number of information-bearing frequency bands. This means that increasing the number of channels results in many observations that only contribute to clutter echo information. Another trade-off is between the bandwidth of the channels and the degree of overlap between channels. If the channel bandwidth is too small, flaw echo information is concealed because of resolution loss. Disproportionate frequency overlap between channels on the other hand, results in excessive correlation among the channels and limits the anticipated TCR improvement. For ultrasonic target detection performance, correlation

is not as critical as choosing the proper frequency range containing significant target echo information.

To achieve the TCR enhancement, which is synonymous with SNR improvement, the SSP method uses a post-processor to combine all of the incoming information from multiple frequency bands. This post-processor reconstructs the time-domain signal with the objective of obtaining maximum TCR. Several types of processors can be used to extract the target echo information. Minimization [9], in particular, is very effective in suppressing the clutter echoes when the target echo information exists in all frequency bands (also known as the observation channels). If too many null-observation channels (or frequency bands in which no target echo information appears because of signal attenuation caused by scattering and absorption) exist, then the minimization processor might not achieve the desired SNR improvement [9]. For example, Fig. 3 exhibits certain channels that do not contain target echo information. Observation channels belonging to low-frequency bands contain target echo information; however target echo information is suppressed in high-frequency bands because of the attenuation effect in high frequencies. Under these circumstances, other post-processing methods such as median or maximization may have more robust detection performance. Minimization, median, and maximization methods are called OS filters. OS concepts have been developed in the statistics field and successfully employed in radar, sonar, and image-processing applications [9], [10].

It is important to note that the SSP-NN system proposed in the paper is a target/flaw echo enhancement system that precedes a detector. Therefore, after the post-processor step, a detector can be used to make a binary decision to determine if a target is present or not. This detector can be designed by using an adaptive thresholding algorithm such as that in [15] for constant false-alarm rate (CFAR) detection.
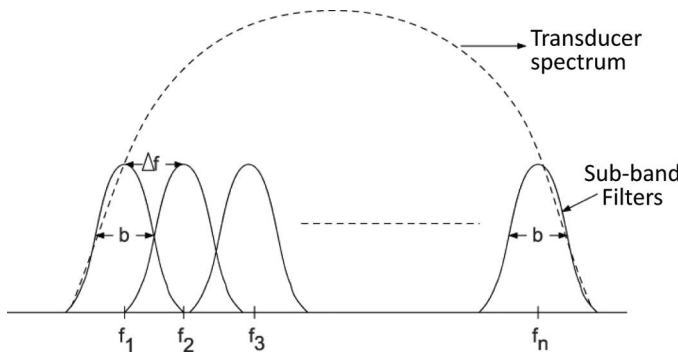

Fig. 2. Frequency bands in split-spectrum processing: b is the filter bandwidth, Δf is the frequency step between successive bands, $f_1, \ldots, f_n$ are the sub-bands' center frequencies.
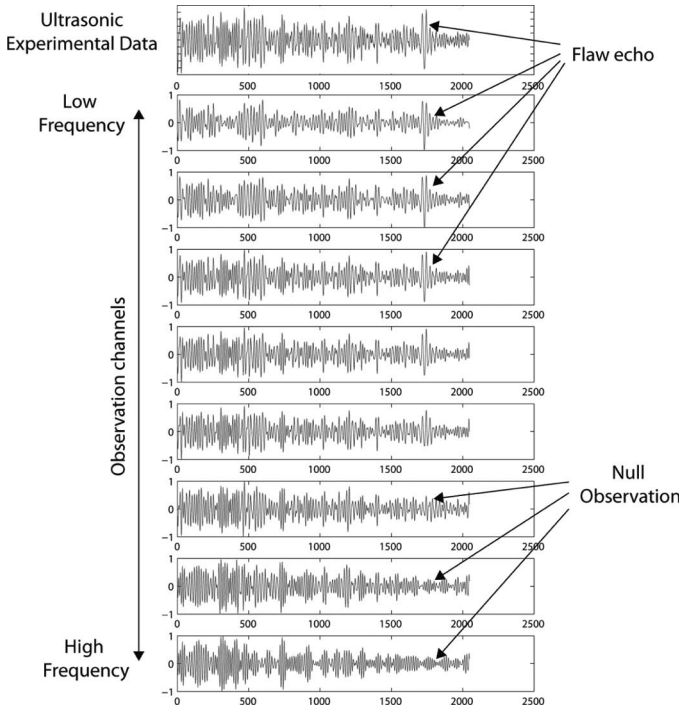
Fig. 3. Observation channels and null observation in higher frequency bands.

Fig. 4. Ultrasonic testing setup using a steel block to evaluate the characteristics of target (hole) echo and grain scattering.

In the following section, the frequency analysis of the ultrasonic signals is presented and the frequency diversity between clutter echoes and target echoes is highlighted. This difference in frequency response can be exploited using a ranked order statistics detection algorithm.

III. Frequency Analysis and Order Statistics of Ultrasonic Signals

In the Rayleigh scattering region, where the wavelength of the interrogation wavelet is much larger than the size of scatterers, microstructure scattering results in an upward shift in the expected frequency of broadband ultrasonic scattering echoes. In this region, the scattering coefficient varies with the average volume of the scatterers and the fourth power of the wave frequency, whereas the absorption coefficient increases linearly with frequency [16]. This is not the case for target echoes because targets are usually larger in size compared with the wavelength of the ultrasonic signal and behave like geometrical reflectors. In fact, target echoes often display a downward shift in their expected frequency which is caused by the overall effect of attenuation governed by the physical properties of the propagation path. This downward frequency shift of the target is a useful attribute because the microstructure scattering noise and target echoes are concurrently received. The exploration of the frequency content of ultrasonic backscattered signals can give spectral energy profiles corresponding to the grains or tissues and the larger reflectors (e.g., defects, delamination, voids, tumors, pathological chan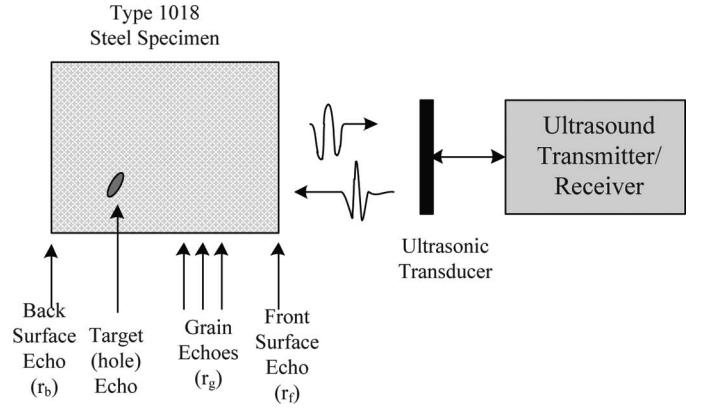ges of tissues, etc.). If the information-bearing frequency bands that are dependent on the specific characteristics of the propagation path are known *a priori*, optimal band-pass filtering can be employed to improve the target visibility [9].

The composite effects of scattering and attenuation caused by microstructure can be characterized in terms of transfer functions derived from the spectra of measured signals. For example, as shown in Fig. 4 for ultrasonic testing of materials using a pulse/echo system, the front-surface echo represents the transfer function of the transducer impulse response, $U(f)$, the pulser, receiver amplifier, and the water propagation path. In the RF frequencies (1 to 15 MHz range), the frequency characteristics of the pulser and receiver amplifier are broad and assumed to be constant for the frequency range of interest, and the water propagation path is frequency independent. Therefore, the transfer function of the received front-surface echo signal is proportional to the broadband transfer function of the ultrasonic transducer impulse response:

$$R_{f}(f) \propto U(f). \qquad (1)$$

The spectrum of the received echo from the back surface of the specimen, $R_{b}(f)$, can be modeled as

$$R_{b}(f) \propto A(f)U(f), \qquad (2)$$

where $A(f)$ is the transfer function corresponding to the attenuation characteristics of the signal propagation path within the specimen. A heuristic evaluation of $A(f)$ can be obtained by the ratio of the spectra of these measured signals, $|R_{b}(f)|/|R_{f}(f)|$. Consequently, there is a definite shift or emphasis of the lower frequencies because the higher frequency components attenuate at much higher rate (attenuation is higher for higher frequencies). This indicates that echoes associated with the defect (i.e., target) in the material, which is significantly greater in size than the wavelength, have dominant energy in lower frequencies. The scattering function, $S(f)$, can be found by the ratios of the expected spectra of the grain echoes, $R_{g}(f)$, and the front surface echo $R_{f}(f)$, $|R_{g}(f)|/|R_{f}(f)|$. Therefore, the

grain scattering causes the lower frequencies to become poorly backscattered (i.e., attenuated) and higher-frequency components are emphasized because the Rayleigh scattering phenomenon emphasizes higher frequency. This phenomenon results in an upward shift in the expected frequency associated with the microstructure scattering echoes. Thus, to take advantage of this property in target detection, frequencies for which the grain scattering is minimal should be emphasized to maximize the TCR. This property can be confirmed directly by inspecting Fig. 3, in which the lower frequency bands exhibit better target visibility.

In certain instances, as discussed previously, both target and scatterers display predictable frequency dynamics associated with the physical properties of the material. These characteristics are advantageous and lead to obtaining an optimal frequency range containing high TCRs for the sub-band decomposition stage of the SSP block diagram shown in Fig. 1. In SSP, after sub-band decomposition, the next step is to use the partially uncorrelated observations and make use of statistical differences in the channels corresponding to random processes inherent to microstructure and target echoes for improved target detection. The statistical differences of microstructure and target echoes can be exploited using OS filters. A ranked OS processor is shown to be a quantile estimator that describes a specific point on the probability distribution function. The performance of the OS-based target detector can be improved [9], [10] by choosing a particular rank with the least overlap between probability density functions of the two hypotheses representing target, H_1, or clutter, H_0.

An important step for optimizing the OS filter involves finding the relationship between the input and output statistical behavior of the data. The OS filter ranks a set of n input values corresponding to simultaneously sampled values of the n channels of the SSP output, $(x_1, x_2, x_3, \ldots, x_n)$,

$$x_{(1)} \leq x_{(2)} \leq x_{(3)} \cdots \leq x_{(n)}, \tag{3}$$

where a given order or rank, r, is chosen and $x_{(r)}$ is passed to the output. This processor is the median filter when $r = (n+1)/2$ (for odd n), the maximum filter when $r = n$ and the minimum filter when $r = 1$. It should be noted that the performance of the OS filter will generally improve with increasing observations n because the variance will decrease (i.e., the random nature of the scattering echoes will be reduced). It can be seen that the parameters r and n can be used so that the OS filter emphasizes particular regions in the distributions of the input signals. The lower-ranked order statistics have been shown in the past to give improvement in the resolution of echoes and the TCR [17], provided all channels have significant target information.

In the next section, we present an alternative post-processing technique based on NNs which offers superior and more robust detection performance because of its trainability and capability to deemphasize the contribution to the decision making process of those sub-band signals with intrinsic null target information.

IV. Neural Network Post Processor

NNs are nonlinear mapping processes that allow training and adaptability for signal classification applications [18]–[21]. The learning process enables NNs to recognize the target patterns without mathematical models of the target signal distributions, which often are unknown. There are several key advantages of NNs: 1) NNs are trained by desired result, which means that no mathematical model is necessary; 2) NNs approximate unknown systems which include non-linear models—this non-linearity is an important property which enhances the network's classification or approximation capabilities without estimating any statistical parameters; and 3) NNs have parallel structure and provide fast computation for real-time target detection applications.

In this study, a three-layer feed-forward NN is used as the post-processor of the ultrasonic target detector. A 3-layer feed-forward NN provides the best compromise between implementation complexity and the SSP performance. A feed-forward NN contains many nodes, and each node consists of a basic computation function and an activation function. A computation unit processes the input signals and sends them to the activation function. The activation function unit produces the output of the node which can be the final output of a NN or the input of another neural node. An objective function is used to train the NNs. The squared error function, which is computed between the output of NNs and the desired output, is used as the objective function. The objective function measures how differently NNs behave from the desired outputs. The goal of the NN learning is to find the weight coefficients for which the objective function reaches the minimum value.

The backpropagation algorithm is used to train a 3-layer feed-forward NN as shown in Fig. 5. The nodes in the first layer forward SSP data to the second layer. The neural nodes in the second layer, which are called hidden-layer nodes, receive the weighted inputs from the first layer and then perform a nonlinear mapping calculation using the activation function. The output neural nodes in the third layer sum up the weighted inputs from second layer. The model of a neural node used in the hidden layer is shown in Fig. 6. The weight coefficients w_{ji} indicate the ith input and jth node.

The general neural node model can be expressed by

$$y_j = \varphi\left(\sum_i w_{ji} x_i + b_j\right), \tag{4}$$

where x_i is a set of inputs of each neuron, y_j is a set of outputs of each neuron, and b_j is a set of bias of each neuron. Each input is multiplied by a weight coefficient w_{ji}. The subscript ji refers to the input i in neuron j. The
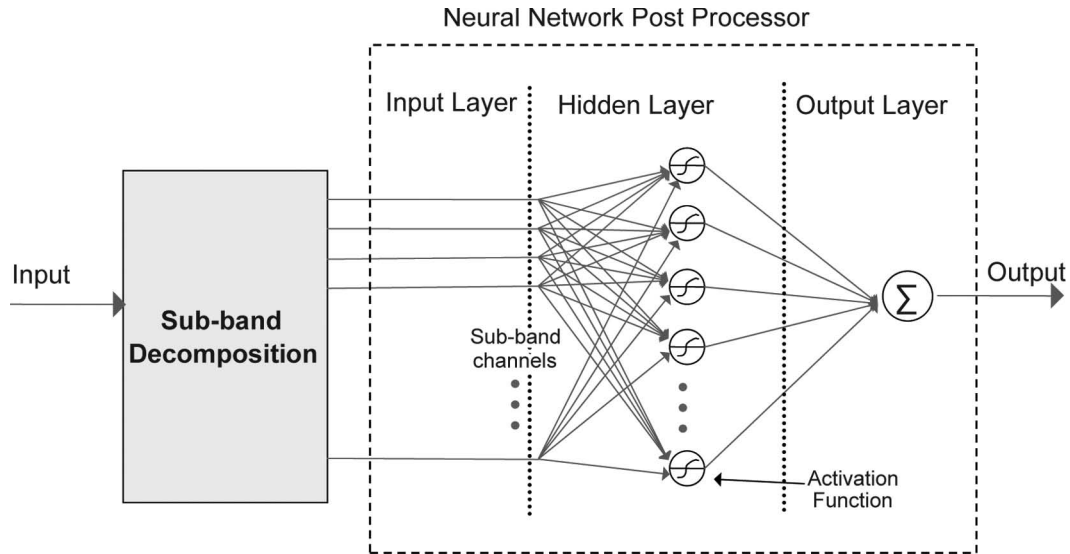
Fig. 5. Three-layer feed-forward neural network for split-spectrum processing target detection.

term φ is an activation function. The activation function of the hidden layer must be differentiable (because the backpropagation algorithm needs the derivative of the activation function during its learning process) to ensure the weights and activations are bounded. Hence, the activation function used in the hidden layer is the sigmoid function, which can be expressed by

$$\varphi(x) = (1 + e^{-x})^{-1}. \tag{5}$$

The learning process allows NNs to adapt to the environment of a particular application. The learning step takes place through iterative process of adjusting weight values using the backpropagation algorithm. In the learning process, it is important to select the initial weights randomly because the training result can be limited to a local minimum based on the initial values. After the training, the weight coefficients are fixed and then used for the other input sets. Additional training for NNs is only necessary when the environments of the application are changed.

To train the NNs for the ultrasonic target detection, we used an experimental ultrasonic signal which has a target echo in *a priori* known location. The desired output data are made of all 0 values for clutter and a 1 value at the known target location. The initial values of weights and bias are randomly selected. The number of input nodes is the same as the number of SSP channels and only one output node is used. It is important to note that the number of hidden nodes affects the performance of the NNs. After numerous performance evaluation trials, we have observed that using 5 hidden neural nodes performs superbly with SNR exceeding 40 dB in detecting a target masked by high density clutter. An objective function such as the sum of the squared error function is necessary to reach the minimization criterion to complete the learning process. If the minimization criterion of the objective function is not met, we increase the number of epochs, which correspond to a single presentation of all patterns in the training set.

If the criterion is still not met with the larger number of epochs, increasing the number of hidden nodes can fix the problem. However, as expected, increasing the number of epochs or hidden nodes requires more training time.

The NN-based SSP target detection system for ultrasonic signals (the target is a flaw in a steel block and clutter represents grain scattering) is implemented in Matlab software (The MathWorks, Natick, MA) for performance evaluation. The ultrasonic experimental signals are used for both training NN and detection tests. Fig. 7 shows the data for training and the desired output data. The backpropagation learning algorithm computes the mean-squared error of the difference between the desired output and real output value and adjusts the weight and bias
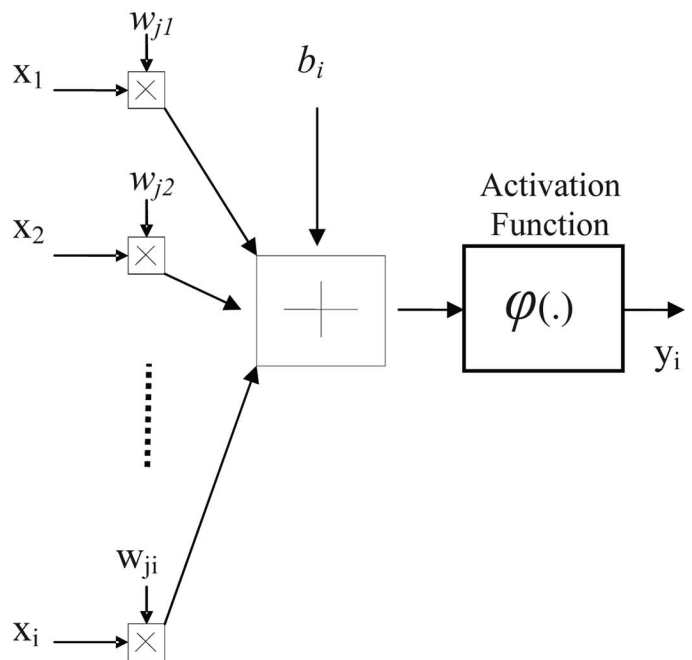

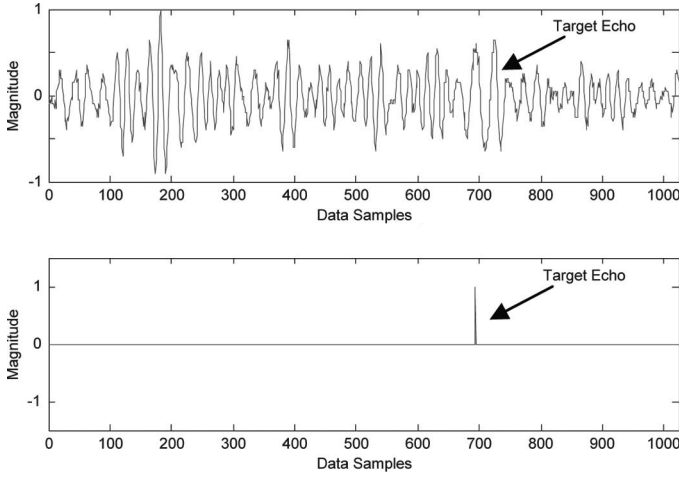Fig. 6. Hidden-layer neural node model.

Fig. 7. (top) Training data and (bottom) desired output.

coefficients until the mean-squared error function reaches the minimum value. After training, the NN is expected to respond to target echoes if the input signal to NN-SSP system contains target information. The NNs provide an impulse corresponding to the location of a target echo and small values for clutter echoes, because during the learning process 1 was assigned to a target echo and 0 was assigned to clutter echoes. In this research, an 8-channel SSP and 5 hidden nodes have been used. The result of trained NN-SSP target echo visibility enhancement is shown in Fig. 8.

For major changes that occur in the experimentation setup (such as using different transducer types, different frequency of interrogation, or change in material types), it may be necessary to re-train NN weight coefficients.

V. TARGET ECHO VISIBILITY ENHANCEMENT PERFORMANCE EVALUATION

The performance of the NN post-processor is measured against other conventional post-processing methods
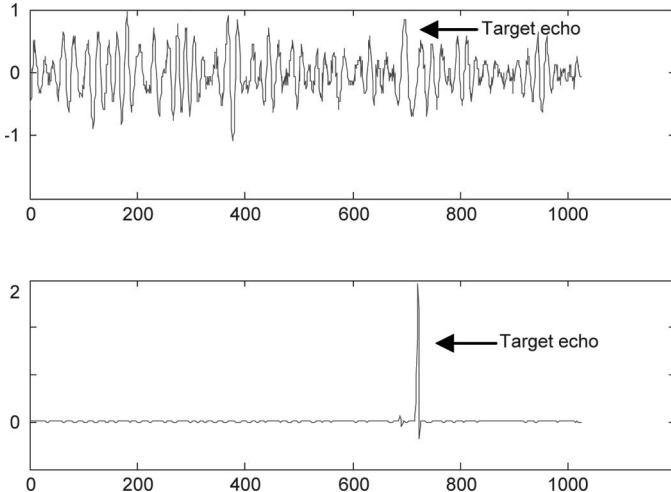

Fig. 8. (top) Experimental data and (bottom) target echo visibility enhancement results using neural network based SSP.

such as averaging, OS (minimum and median), geometric mean [22], and polarity detectors [23]. The mathematical expressions of these techniques are given as follows: average detector:

$$\phi_{\mathrm{av}}(n) = \frac{1}{k}\sum_{j=1}^{k}|z_j(n)|, \tag{6}$$

median detector:

$$\phi_{\mathrm{med}}(n) = \mathrm{median}[|z_j(n)|, \quad j = 1, 2, ..., k], \tag{7}$$

minimum detector:

$$\phi_{\mathrm{min}}(n) = \mathrm{min}[|z_j(n)|, \quad j = 1, 2, ..., k], \tag{8}$$

geometric mean detector:

$$\phi_{\mathrm{gm}}(n) = \sqrt[k]{\prod_{j=1}^{k}|z_j(n)|}, \tag{9}$$

polarity detector:

$$\phi_{\mathrm{p}}(n) = \begin{cases} z(n) & \begin{array}{l}\text{if } z_j(n) > 0 \text{ or } z_j(n) < 0 \\ \text{for all } j = 1, 2, ..., k\end{array} \\ 0 & \text{otherwise,} \end{cases} \tag{10}$$

where z_j is the SSP output of channel j, and k is the total number of the SSP channels.

The NNs and other detection methods are implemented and compared with experimental ultrasonic data. For performance analysis and testing, the experimental A-scan data from a steel block (type 1018, grain size 50 μm) are acquired and analyzed. A Panametrics (type 5052, Panametrics Inc., Waltham, MA) pulser/receiver is used to drive the ultrasonic transducers and to receive the ultrasonic backscattered echoes. The received echo signals are then converted to digital data for split-spectrum processing. The A-scan measurements were conducted using a broadband ultrasonic transducer of 0.5 in (1.27 cm) diameter with 5 MHz center frequency. Data were acquired with a 100 MHz sampling rate and each sample is 8 bits. 1024 data points for each A-scan represents approximately a depth of 2.5 cm. The steel block has several defects (holes of 1.5 mm diameter) at known, separate locations. All of the A-scan measurements probe the hole (target) positions within the steel block. For performance analysis, TCR is evaluated by finding the maximum target echo amplitude after the post-processing step. This value is compared with the largest amplitude of clutter echoes. Therefore, TCR can be defined as

$$\mathrm{TCR} = 20 \times \log_{10}(T/C), \tag{11}$$

where T is the maximum target echo amplitude and C is the maximum clutter echo amplitude.

Fig. 9 shows experimental data in the time domain [Fig. 9(a)] and frequency domain [Fig. 9(b)] as well as the

frequency spectra of the 8-channel SSP band-pass filters [Fig. 9(c) and Fig. 9(d)]. Fig. 9(c) covers the frequency range where the flaw echo exists in all sub-bands (no null observations). Fig. 9(d) shows the frequency spectra of the 8 sub-band filters which cover the full frequency spectrum of the signal. In this case, some sub-band filter outputs (higher-frequency bands) may have very low TCR and are considered to be null observations. Therefore, a robust target detection method which offers minimal sensitivity to the frequency coverage of filters is desirable. The comparison results of various detectors applied to SSP channels covering the low-frequency region (ranging from 1.5 to 6 MHz) are shown in Fig. 10. In this frequency region, there are no null observations. With the NN detector, the target (hole) echo is sharply detected without evidence of noticeable clutter. The other detectors also detect the target. Table I also confirms that the NN outperforms the other techniques. The average TCR of the NN detector is 46.8 dB; however, the average TCR of the minimum detector is 7.9 dB. The TCRs of the other detectors are significantly lower than the minimum detector.

Fig. 11 shows the comparison results of various techniques applied to SSP channels covering the full frequency spectrum (ranging from 1.5 to 9 MHz) of the ultrasonic data. It is important to point out that null observations exist in this frequency range. NNs can still enhance the flaw echo visibility; whereas the other techniques fail to distinguish the presence of the flaw echo. In Figs. 10 and 11, NN output values are close to 0 for clutter echoes and close to 1 for target echoes. For other OS filters, output values are normalized to −1 and 1 for presentation purposes.

Tables I and II show the FCR results of the original input data and six different post-processors with two different sub-band filters' coverage. These results confirm that the NN processor not only outperforms the conventional methods but also shows less vulnerability to null-observations.

For a binary detection operation, a thresholding step can be applied to the NN-SSP results. It can be seen from experimental results that the amplitude difference between a target echo and clutter echoes is in the range of several orders of magnitudes. When there is no target in the A-scan input, the processed output values are very close to 0 (do not reach more than 0.01). Therefore, a threshold value such as above 0.01 can be used for detector operations. As an alternative to this approach, adaptive threshold values can be used; this issue has been addressed in [15].

In the next section, we present an FPGA-based hardware platform for real-time ultrasonic target detection applications. Architecture details and implementation results are discussed.

VI. SSP-NN System Architecture

The SSP-NN ultrasonic target detection system, as shown in Fig. 5, is implemented with eight inputs, five hidden nodes, and one output node. Each hidden node block receives every eight-channel output of SSP and processes the input data with weight coefficients and bias. Each hidden node has different weight coefficients and bias from the other hidden nodes. The values of the weight and bias coefficients are calculated off-line using Matlab and stored in the memory of FPGA. It is not necessary to reload these coefficients during the ultrasonic target detection process unless the test environments are changed.

Many different architectures are feasible to implement NNs in hardware. One effective architecture is the design of reconfigurable processing elements, which allows the NNs to be reorganized and reconfigured by adjusting the number of hidden nodes and their associated weight coefficients [24], [25]. This reconfigurable architecture provides flexibility and adaptability not only in design with FPGA, but also in application-specified integrated circuit (ASIC) design. An alternate improvement over the reconfigurable design is parallel architecture which can be optimized for high-speed operation and high throughput using pipelined and concurrent multiplications and additions. Pipelined architecture tolerates a high-speed clock rate at the expense of additional hardware resources, especially multipliers and adders.

The SSP-NN system is realized using a Nallatech XtremeDSP kit [26], [27] (Nallatech, Lanarkshire, UK) with a Xilinx Virtex-4 device [28] (Xilinx Inc., San Jose,
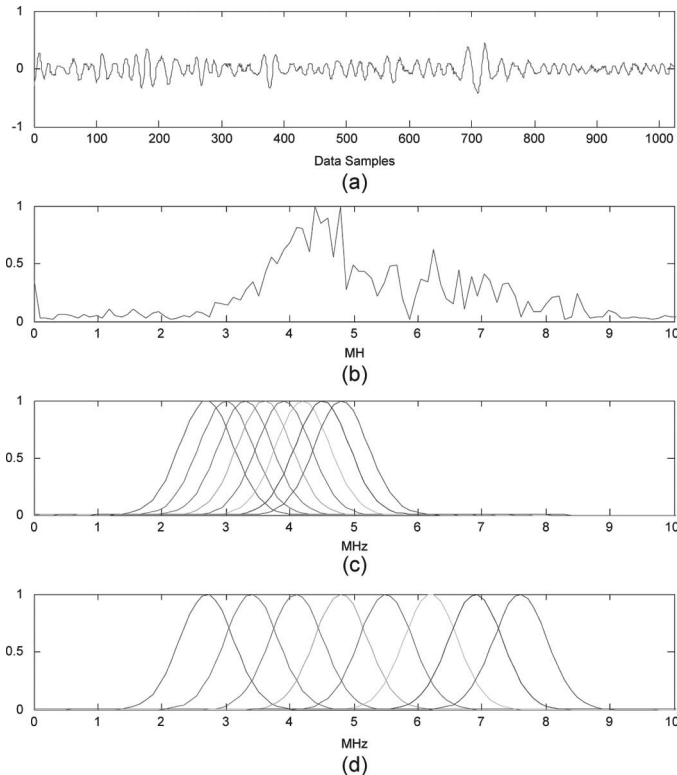

Fig. 9. Experimental data in (a) time domain and (b) frequency domain, (c) split-spectrum processing (SSP) filter locations covering the low-frequency region, and (d) SSP filter locations covering the full frequency range.

TABLE I. TCR ENHANCEMENT OF VARIOUS SPLIT-SPECTRUM PROCESSING (SSP) POST-PROCESSING TECHNIQUES
WHEN SSP FILTERS COVER THE LOW-FREQUENCY REGION OF THE SIGNAL.

Trial number	Input TCR (dB)	Neural networks detector (dB)	Minimum detector (dB)	Median detector (dB)	Average detector (dB)	Geometric mean detector (dB)	Polarity threshold detector (dB)
1	2.2	41.7	9.2	5.4	5.2	6.1	0.1
2	0.0	44.6	6.5	6.6	4.1	5.9	0.1
3	1.5	47.1	7.3	8.2	6.0	6.9	0
4	2.7	55.4	5.7	5.8	2.8	6.6	0
5	0.0	45.5	5.0	7.8	5.0	7.7	0
6	0.0	46.7	13.6	8.9	7.0	9.2	0
Mean	1.1	46.8	7.9	7.1	5.0	7.0	0
STD	1.2	4.6	3.1	1.4	1.5	1.2	0

CA). The Virtex-4 device provides 192 DSP slices and the board has an analog-to-digital converter (ADC) which can sample the signal with a sampling rate of up to 105 mega samples per second. A hardware-efficient piecewise linear approximation of a nonlinear (PLAN) function [29] is used to realize the hardware for the sigmoid function blocks. In the PLAN method, the sigmoid function is made of various straight lines. The complexity of computing the nonlinear approximations is reduced by choosing a shifter instead of a multiplier. The shift and add operations are
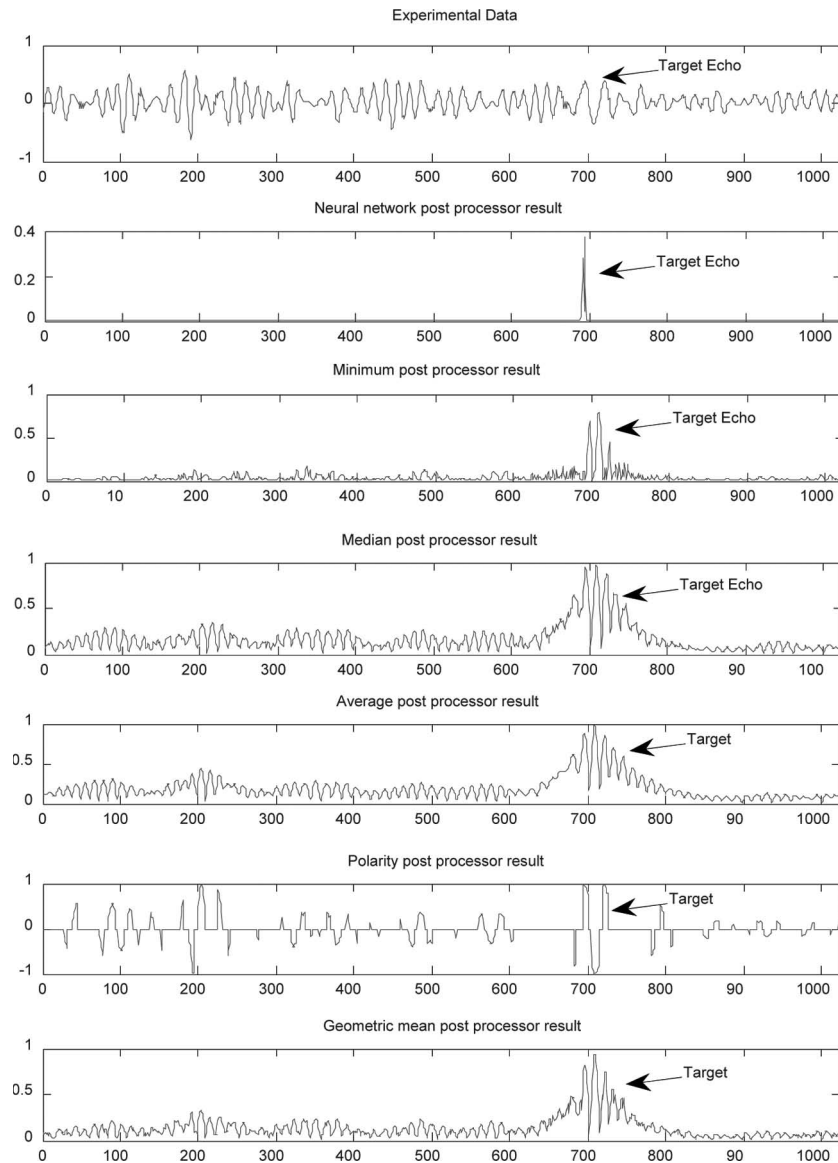

Fig. 10. Comparison of target echo visibility enhancement results when split-spectrum processing channels are covering the low-frequency region.

TABLE II. TARGET-TO-CLUTTER RATIO (TCR) ENHANCEMENT OF VARIOUS SPLIT-SPECTRUM PROCESSING (SSP) POST-PROCESSING
TECHNIQUES WHEN SSP FILTERS COVER THE FULL FREQUENCY RANGE OF THE SIGNAL.

Trial number	Input TCR (dB)	Neural networks detector (dB)	Minimum detector (dB)	Median detector (dB)	Average detector (dB)	Geometric mean detector (dB)	Polarity threshold detector (dB)
1	2.2	26.3	0	0	1.7	0	1.1
2	0.0	44.6	4.7	0	0.8	1.6	0
3	1.5	22.5	0	2.6	2.5	2.3	0
4	2.7	22.2	2.8	0	1.5	2.5	0
5	0.0	13.6	0	0	0	0	0
6	0.0	16.9	2.4	3.3	2.0	2.4	1.0
Mean	1.1	23.7	1.7	1.0	1.4	1.5	0.3
STD	1.2	10.8	2.0	1.5	0.9	1.2	0.5

implemented with minimal logic gates. In the NN design, a total of five hidden-node processing blocks are used for concurrent computation. As shown in Fig. 12, each hidden node has eight multipliers, corresponding to the output of 8 SSP channels, eight adders, and one sigmoid function block. Fig. 13 shows the diagram of the output node. The output node is composed of five multipliers and five adders. This design has a total of 45 multipliers and 12 pipelined group delays. It takes 8-bit input, 18-bit weight coefficients, and provides 27-bit output. This architecture of the NN block has been tested for a 1024-point data set with 8-channel SSP modules operating with a 100-MHz clock. The total execution time of the NNs block is 10.36 µs.

The host platform for the SSP-NN ultrasonic target detection system, Nallatech XtremeDSP, has three Xilinx FPGAs, ADC, and a digital-to-analog converter (DAC). The top-level diagram of the system is shown in Fig. 14. All modules of the ultrasonic target detection system are implemented in a Xilinx Virtex-4 FPGA which is the main
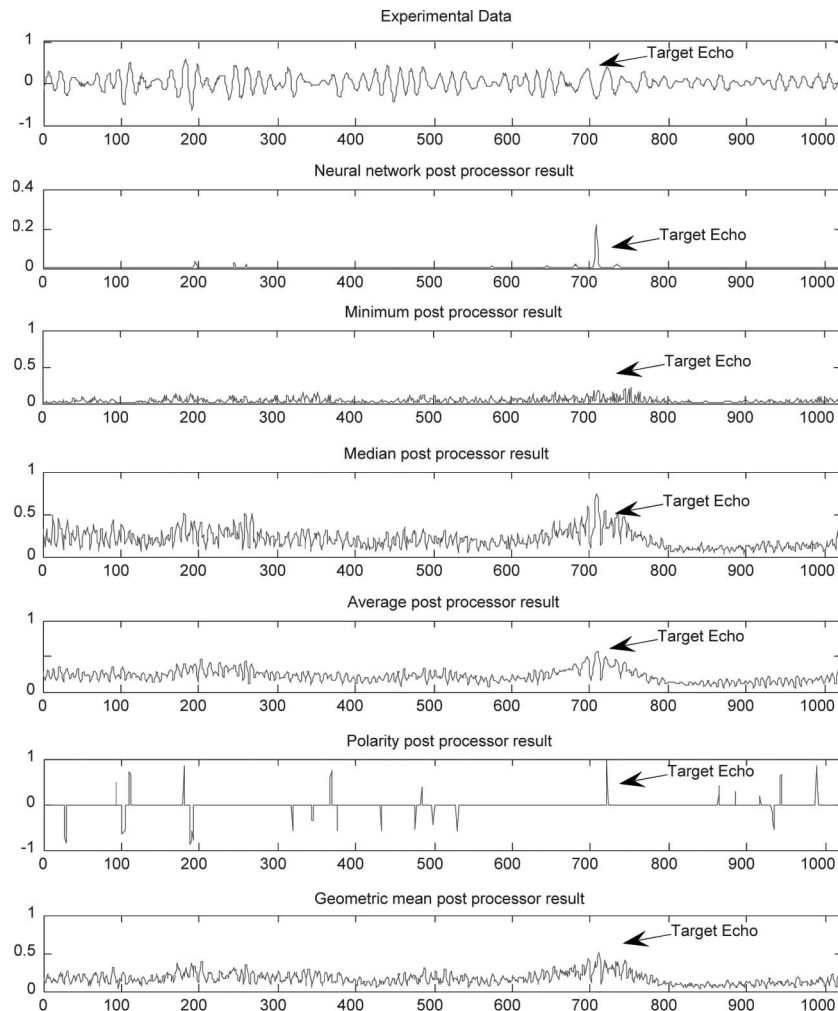

Fig. 11. Comparison of target echo visibility enhancement results when split-spectrum processing channels are covering the full frequency range.
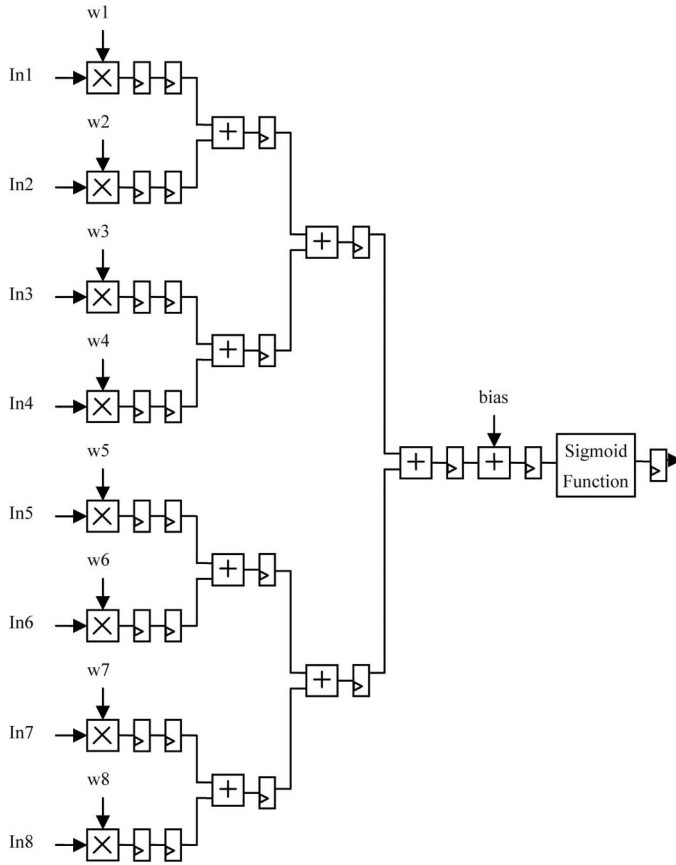
Fig. 12. Hidden node architecture, where In1 to In8 are the output of an 8-channel split-spectrum processing module.

Fig. 13. Output node architecture where In1 to In5 are the output of the 5 hidden nodes.

user FPGA of the Xtreme DSP development kit [26]. A Xilinx Virtex-II FPGA is used for clock management and also provides the sampling clock to ADCs and DACs. The other FPGA, Xilinx Spartan-II, is used for the PCI/USB interface. This device is pre-configured for PCI/USB communication with the host computer. The Matlab GUI program has been developed to control the Nallatech DSP kit through the USB interface. The Nallatech DSP kit also provides two Analog Devices ADC chips (AD6645, Analog Devices Inc., Norwood, MA) and two Analog Devices DAC chips (AD9772A). These chips are used to control the transducer and capture the input ultrasonic experimental data. The ADC chip can accept a maximum of 2 Vpp ultrasonic signals and convert the input signal to 14-bit data with a sampling rate of up to 105 MHz.

The SSP-NN ultrasonic target detection system is composed of a data capture block, a signal processing block, and a communication block for the host computer:

- The data capture block gathers the incoming data from the ADC and controls the excitation timing of the transducer. This block has a different clock domain, allowing the processing block to work at a clock rate independent of the ADC sampling rate.
- The signal processing block has four submodules: the SSP module, the normalization module, the control module, and the NN post-processing module.
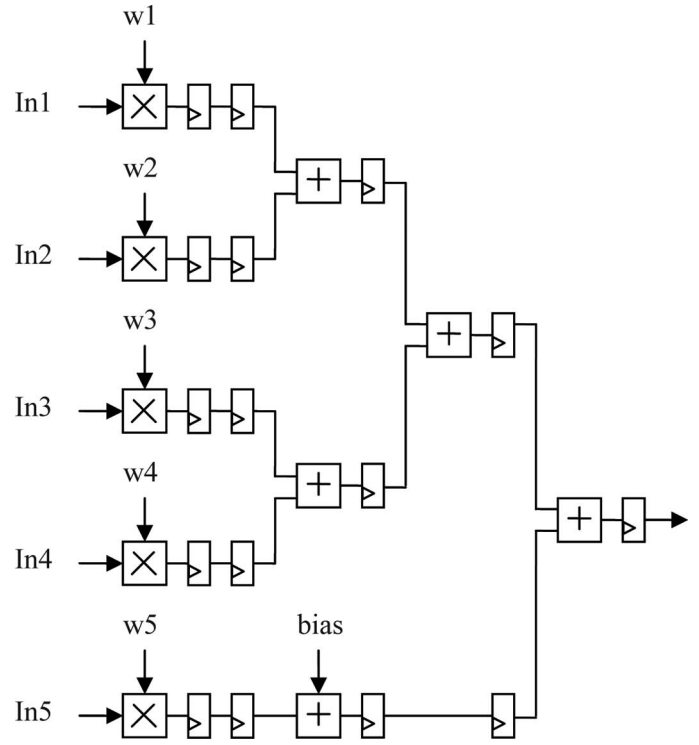
- The communication block provides the interface to the host computer. With this block, we can access the register map to control the system and the DMA interface connected to internal dual port Block RAMs (BRAM) for computational results.

Fig. 15 shows the functional diagram of the signal processing block. This block consists of an FFT module, sub-band
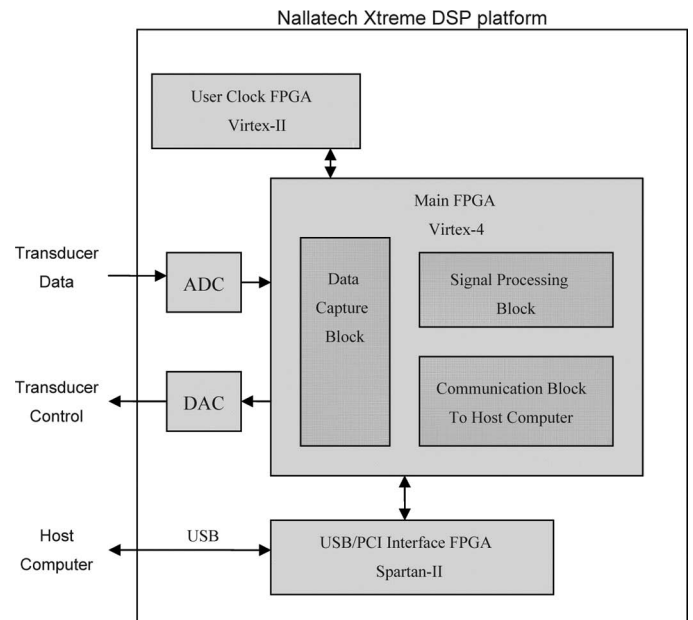

Fig. 14. The functional block diagram of the split-spectrum processing–neural network ultrasonic target detection system.
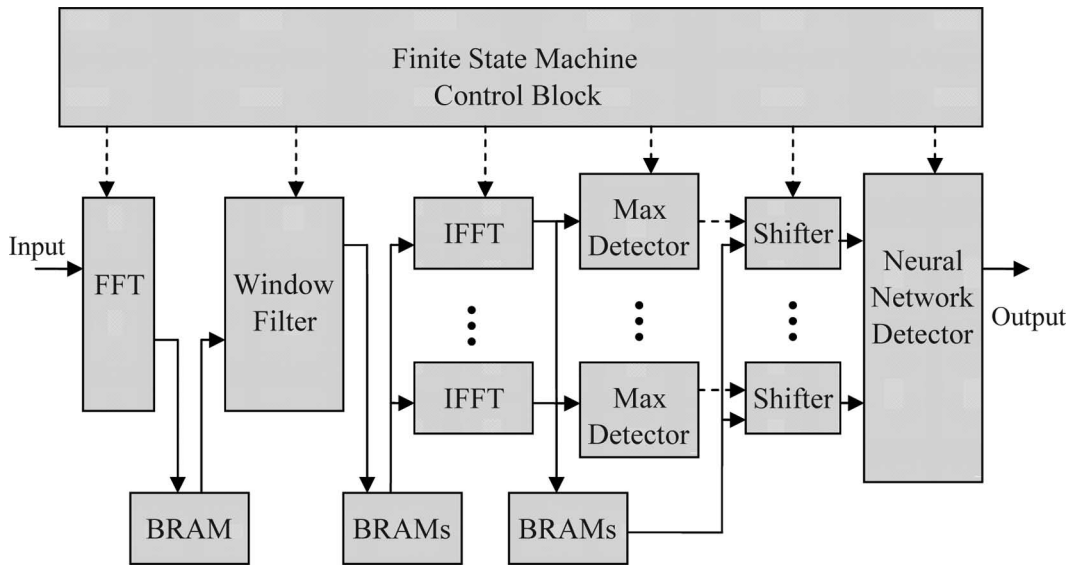
Fig. 15. The block diagram of the signal processing block.

filters, IFFT modules, and BRAMs. The FFT module is Radix-2 IP provided by Xilinx [30]. This FFT IP is highly optimized for speed and area using a dedicated DSP block in Xilinx Virtex-4 FPGA. The FFT IP is generated with 8-bit inputs and 19-bit outputs. The FFT outputs are truncated to a 16-bit precision for the rest of the design.

Ideal sub-band filters (i.e., rectangular window for sub-band partitioning of a measured broadband signal) are used for implementation to reduce the required hardware resources. In our experiments, we found minor performance loss (1 to 2 dB) with the windowing method; however this loss is insignificant because the target-to-clutter improvement is more than 40 dB, as shown in Tables I and III.

The NN detection blocks are also trained with rectangular windows for splitting the spectrum. The rectangular window SSP can be controlled by the three following parameters: the starting frequency of the first band, bandwidth, and the extent of frequency overlap from band-to-band. The performance of the ultrasonic target detector is highly dependent on these parameters. These SSP parameters are controlled by the host computer without requiring the reconfiguration of the FPGA.

The normalization module includes two submodules which are the maximum detector and barrel shifter. The maximum detector determines the maximum value of each channel of SSP and controls the barrel shifter to adjust the magnitude of SSP outputs. The finite-state machine control module governs the sequence of operations of all processing blocks. The NN module is used for the post-processing block. The weights and bias coefficients are pre-calculated using Matlab and stored in the memory of the FPGA. These coefficients are determined during the training using the rectangular window SSP and experimental ultrasonic data. The desired output set of learning algorithm is made of all zero for clutter signal and an im-

pulse for the target echo. This processing block operates at a 100 MHz clock rate.

The weight and bias coefficients must be carefully calculated for hardware implementation because the coefficients are 18-bit fixed point numbers. In this hardware implementation of the NN block, all computation units and coefficients use fixed-point number procedures, although Matlab software uses floating-point computations. During the learning process, weight and bias coefficients values are not limited. However, these coefficients must be limited based on the maximum value of the fixed-point number. In addition, the bias coefficients are critical for bit-shift scaling based on the point location of the input data and weight coefficients. Once the learning process is complete, the maximum coefficients are compared with the maximum value of the fixed-point number. If the maximum coefficients values are in the range of the fixed-point number, the coefficients are chosen for the hardware implementation. If the maximum coefficients are not within the fixed-point bit range, the learning process will run again until the range criteria are met. These scaling and selecting processes are done by the Matlab software. This prevents overflow during the fixed-point computation.

VII. System Operation and Performance Evaluation

The operation of the SSP-NN target detection system is controlled by a host computer through a graphical user interface (GUI) software using Matlab. The dashboard for the GUI software is shown in Fig. 16. This software facilitates controlling the designed modules within the FP-GAs. The system can process ultrasonic data inputs from two different sources. The first one is data input from the transducer in real time. In this case, a pulse generator

TABLE III. TARGET-TO-CLUTTER RATIO (TCR) RESULT COMPARISON BETWEEN NEURAL
NETWORKS AND MINIMIZATION.

Trial number	Input FCR (dB)	Neural networks detector (dB)	Minimum detector (dB)
1	3.69	45.40	6.71
2	−2.33	39.82	9.98
3	2.24	42.33	10.97
4	−3.74	38.26	6.37
5	0	43.42	7.31
6	1.537	36.68	8.96
Mean	0.23	40.98	8.38

module controls the trigger pulse to excite the transducer for pulsing. It also controls the capture of ultrasonic input data from the ADC chip. The second input type is from the host computer using the experimental ultrasonic data already captured. The GUI panel allows the control of SSP filter bandwidth, overlap, and start frequency in real time. The GUI software displays six different figures showing the stored results in the internal dual-port memory (BRAMs). Two figures are designated to display the input and the processed output signals. The remaining four figures can be dynamically controlled by the GUI. These figures can display the data of any internal memory which has sub-band signals. The other function of GUI is to calculate TCR (or SNR) performance of the input and output data.

Table III shows the TCR performance results of hardware implementation for NNs and minimum detectors with 8-channel SSP. The hardware implementation of the NNs detector shows an average 40 dB TCR improvement. However, the minimum detector provides around 8 dB TCR improvement under the same processing conditions. Figs. 17 and 18 also show the superior detection results of hardware-implemented NNs. In particular, Fig. 18 shows the detection of two adjacent targets with NNs. Other detection techniques fail to distinguish multiple targets in close proximity; however NN provides a clear detection and separation of multiple targets.

FFT intellectual property (IP) uses 8-bit input Radix-2 architecture and IFFT IP uses 16-bit input Radix-2 architecture. The input data of FFT and IFFT are truncated
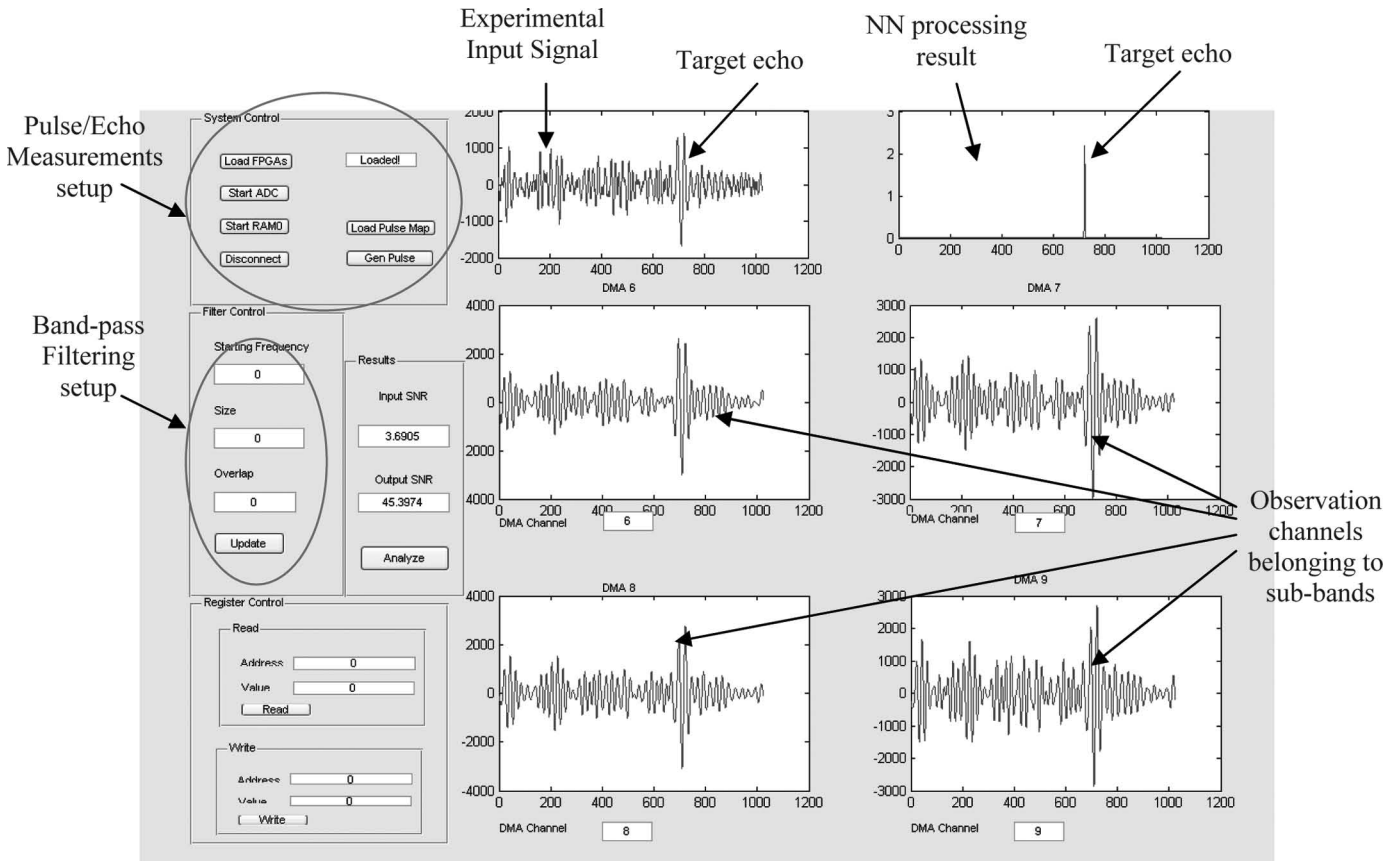

Fig. 16. Graphical user interface for split-spectrum processing–neural network ultrasonic system.
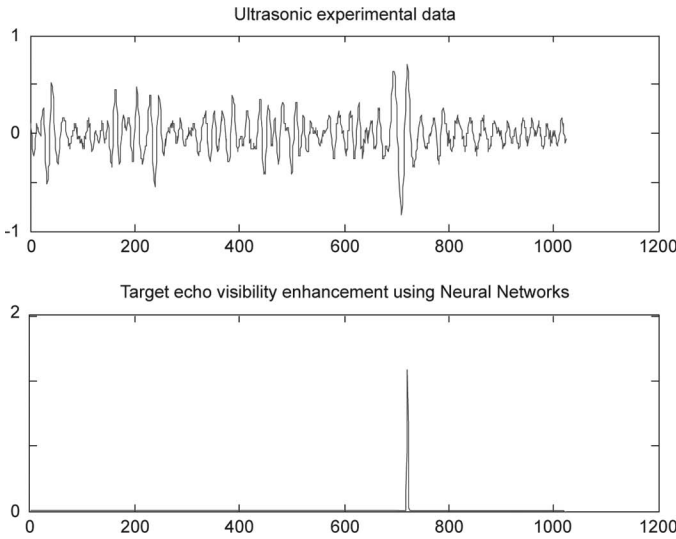
Fig. 17. (top) Ultrasonic experimental data and (bottom) the target echo visibility enhancement result using hardware implementation of neural networks post processor.
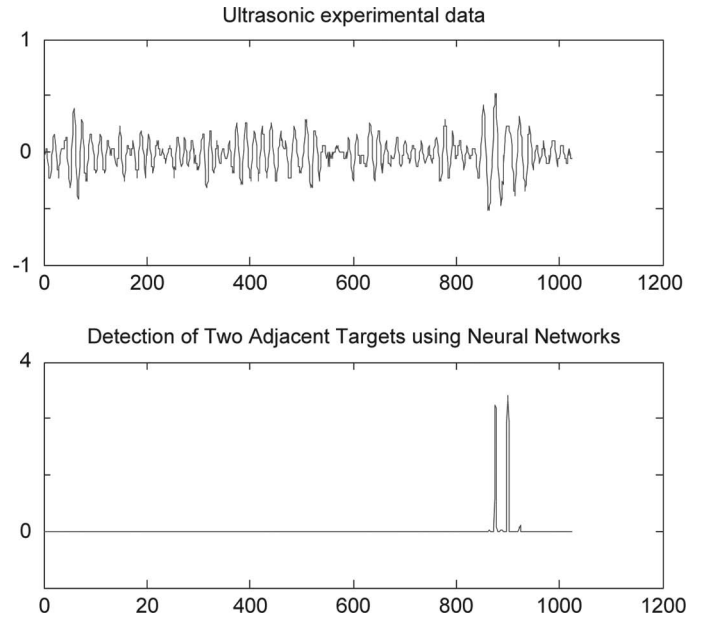

Fig. 18. (top) Ultrasonic experimental data and (bottom) the detection of two adjacent targets using hardware implementation of neural networks post processor.

to 8-bit or 16-bit data. This truncation generates the noise in the output signal. Increasing the precision of FFT and IFFT can reduce the truncation noise. However, the impact of this noise is relatively smaller than the overall noise level and increasing the precision will increase the hardware resource usage.

The main user FPGA, the Virtex-4 device, provides different types of resources such as logic slice, block RAM (BRAM), and DSP48. The logic slice can be configurable to logics, arithmetic operations, and distributed memory blocks. Block RAM provides large storage on the FPGA. In a Virtex-4 device, a BRAM has 18 kB of memory. A DSP48 slice has an 18×18 bit two's-complement multiplier followed by a 48-bit adder. It also supports programmable pipelining and a high-speed path between DSP48 slices. These features allow high-speed cascade operation on FPGA. An NN block can take an advantage of these features because the parallel architecture of NN uses pipelined cascade multipliers and adders. Table IV shows the comparison of resource usage between the NN and minimum detectors. The NN detector uses 16% more logic slices and 98% more DSP48s compared with the minimum detector. However, the NN target detector offers over 400% greater improvement in TCR over the minimum detector, and this is a highly desirable property.

The total execution time is an important feature for a real-time processing system. The total processing time is calculated from captured input data to the output of

the post-processor. This time value does not include the input data capturing time and the communication time between host computer and test board. The goal of the total processing time is achieving about 1ms per A-Scan which is equivalent 1000 processed A-Scans every second. Table V shows the processing time comparison between NN and minimization. In this table, a 1024-point data set is used as an A-scan data. All sub-band channels of SSP are processed concurrently using the same number of IFFT blocks as the number of SSP channels. This implies that the total processing time is not dependent on the number of SSP sub-band channels. Both NNs and minimum detectors need about 124 µs processing time per A-scan, which is equivalent to real-time processing of more than 8000 A-scans per second.

VIII. Conclusion

This paper presents the theory and application of combined NNs and split-spectrum processing techniques in ultrasonic target detection applications. Frequency diver-

TABLE IV. Comparison of Resource Usage Between Neural Network and Minimization Systems.

	Neural network	Minimization
Logic slices	16 848	14 505
DSP48	99	54
RAM16	106	106

TABLE V. Field-Programmable Gate Array Processing Time Between Neural Network and Minimization Systems.

Processing step	Neural networks (cycles)	Minimization (cycles)
FFT	5190	5190
Window filtering	1024	1024
IFFT	5190	5190
Post processing	1036	1024
Total cycles	12 440	12 428
Total time	124.40 µs	124.28 µs

FFT = fast Fourier transform; IFFT = inverse fast Fourier transform.

sity of microstructure scattering and target echoes suggest that OS and NN post-processors can be used for target echo visibility enhancement. When statistical information in the observations deteriorates (e.g., null observations) NN post-processors perform more robustly and are far superior to conventional systems. Furthermore, a case study demonstrates that FPGA-based embedded systems are capable of real-time realization of an SSP-NN system for ultrasonic testing applications.

REFERENCES

[1] E. Beasley and E. Ward, "A quantitative analysis of the sea clutter decorrelation system with frequency agility," *IEEE Trans. Aerosp. Electron. Syst.*, vol. 4, no. 3, pp. 468–473, 1968.

[2] G. Lind, "Measurement of sea clutter correlation with frequency radar," *Philips Telecommun. Rev.*, vol. 29, no. 1, 1970.

[3] H. Ray, "Improving radar range and angle detection with frequency agility," in *Proc. 11th IRE East Coast Conf. Aerospace and Navigation Electronics*, 1964, pp. 1361–1367.

[4] B. Gustafson and B. As, "System properties of jumping-frequency radars," *Philips Telecommun. Rev.*, vol. 25, no. 1, pp. 70–76, 1964.

[5] D. K. Barton, *Frequency Agility and Diversity*, Radars, vol. 6, Norwood, MA: Artech House, 1977.

[6] N. M. Bilgutay, J. Saniie, V. Newhouse, and E. S. Furgason, "Flaw-to-grain echo enhancement," in *Proc. Int. Ultrasound Conf.*, 1979, pp. 152–157.

[7] V. Newhouse, N. M. Bilgutay, J. Saniie, and E. Furgason, "Flaw-to-grain echo enhancement by split-spectrum processing," *Ultrasonics*, vol. 20, no. 2, pp. 59–68, 1982.

[8] J. Saniie, K. Donohue, and N. M. Bilgutay, "Order statistic filters as postdetection processors," *IEEE Trans. Acoust. Speech Signal Process.*, vol. 38, no. 10, pp. 1722–1732, 1990.

[9] J. Saniie, D. Nagle, and K. Donohue, "Analysis of order statistic filters applied to ultrasonic flaw detection using split spectrum processing," *IEEE Trans. Ultrason. Ferroelectr. Freq. Control*, vol. 38, no. 2, pp. 133–140, 1991.

[10] J. Saniie and D. Nagle, "Analysis of order statistic CFAR threshold estimators for improved ultrasonic flaw detection," *IEEE Trans. Ultrason. Ferroelectr. Freq. Control*, vol. 39, no. 5, pp. 618–630, 1992.

[11] J. Saniie and D. Nagle, "Pattern recognition in the ultrasonic imaging of reverberant multilayered structures," *IEEE Trans. Ultrason. Ferroelectr. Freq. Control*, vol. 36, no. 1, pp. 80–92, 1989.

[12] J. Saniie, T. Wang, and X. Jin, "Performance evaluation of frequency diverse Bayesian ultrasonic detection," *J. Acoust. Soc. Am.*, vol. 91, no. 4, pp. 2034–2041, 1992.

[13] D. Nagle and J. Saniie, "Performance analysis of linearly combined order statistic CFAR detectors," *IEEE Trans. Aerosp. Electron. Syst.*, vol. 31, no. 2, pp. 522–532, 1995.

[14] P. Weber and S. Haykin, "Ordered statistic CFAR processing for two parameter distributions with variable skewness," *IEEE Trans. Aerosp. Electron. Syst.*, vol. 21, no. 6, pp. 819–821, 1985.

[15] J. Saniie and D. T. Nagle, "Analysis of order-statistic CFAR threshold estimators for improved ultrasonic flaw detection," *IEEE Trans. Ultrason. Ferroelectr. Freq. Control*, vol. 39, no. 5, pp. 618–630, 1992.

[16] E. P. Papadakis, "Ultrasonic attenuation caused by scattering in polycrystalline metals," *J. Acoust. Soc. Am.*, vol. 37, no. 4, pp. 703–710, 1965.

[17] N. M. Bilgutay and J. Saniie, "The effect of grain size on flaw visibility enhancement using split-spectrum processing," *Mater. Eval.*, vol. 42, no. 6, pp. 808–814, 1984.

[18] R. O. Duda, P. E. Hart, and D. G. Stork, *Pattern Classification*. New York, NY: Wiley-Interscience, 2001.

[19] S. Haykin, *Neural Networks*. Piscataway, NJ: IEEE Press, 1994.

[20] A. Tirakis, "Efficient image classification using neural networks and multiresolution analysis," in *IEEE Int. Conf. Acoustics, Speech and Signal Processing*, 1993, pp. 641–644.

[21] C. H. Chen, "On the relationships between statistical pattern recognition and artificial neural networks," in *IEEE Int. Conf. System, Man and Cybernetics*, 1990, pp. 182–183.

[22] J. Xin, K. D. Donohue, N. M. Bilgutay, and X. Li, "Frequency-diverse geometric- and arithmetic-mean filtering for ultrasonic flaw detection," *Mater. Eval.*, vol. 49, no. 8, pp. 987–992, 1991.

[23] N. M. Bilgutay, U. Bencharit, and J. Saniie, "Enhanced ultrasonic imaging with split-spectrum processing and polarity thresholding," *IEEE Trans. Acoust. Speech Signal Process.*, vol. 37, no. 10, pp. 1722–1732, 1989.

[24] S. Yoon, E. Oruklu, and J. Saniie, "Dynamically reconfigurable neural network hardware design for ultrasonic target detection," in *IEEE Ultrasonics Symp.*, 2006, pp. 1377–1380.

[25] S. Yoon, E. Oruklu, and J. Saniie, "Performance evaluation of neural network based ultrasonic flaw detection," *IEEE Ultrasonics Symp.*, 2007, pp. 1579–1582.

[26] Nallatech. (2011, Jan.). XtremeDSP, Development Kit-IV User Guide. Lanarkshire, UK. [Online]. Available: http://www.xilinx.com/support/documentation/boards_and_kits/ug_xtremedsp_devkitIV.pdf

[27] Xilinx Inc. (2011, Jan.). ExtremeDSP for Virtex-4 FPGAs: User guide. San Jose, CA. [Online]. Available: http://www.xilinx.com/support/documentation/user_guides/ug073.pdf

[28] Xilinx Inc. (2011, Jan.). Virtex-4 User Guide. San Jose, CA. [Online]. Available: http://www.xilinx.com/support/documentation/user_guides/ug070.pdf

[29] H. Amin, K. M. Curtis, and B. R. Hayes-Gill, "Piecewise linear approximation applied to nonlinear function of a neural network," *IEEE Proc. Circuits Devices Syst.*, pp. 313–317, 1997.

[30] Xilinx Inc. (2011, Jan.). LogiCORE IP Fast Fourier Transform v8.0. San Jose, CA. [Online]. Available: http://www.xilinx.com/support/documentation/ip_documentation/ds808_xfft.pdf

Jafar Saniie (S'80–M'81–SM'91–F'10) was born in Iran on March 21, 1952. He received his B.S. degree in electrical engineering from the University of Maryland in 1974. He received his M.S. degree in biomedical engineering in 1977 from Case Western Reserve University, Cleveland, OH, and his Ph.D. degree in electrical engineering in 1981 from Purdue University, West Lafayette, IN. In 1981, Dr. Saniie joined the Department of Applied Physics, University of Helsinki, Finland, to conduct research on photothermal and photoacoustic imaging. Since 1983, he has been with the Department of Electrical and Computer Engineering at the Illinois Institute of Technology, where he is a Filmer Endowed Professor, Associate Chair, and Director of the Embedded Computing and Signal Processing (ECASP) Research Laboratory.

Dr. Saniie's research interests and activities are in ultrasonic signal and image processing, statistical pattern recognition, estimation and detection, embedded digital systems, digital signal processing with field-programmable gate arrays, and ultrasonic nondestructive testing and imaging. In particular, he has performed extensive work in the areas of frequency-diverse ultrasonic flaw detection techniques, embedded signal processing architectures and system-on-chip design for ultrasonic imaging, ultrasonic data compression, nonlinear signal processing in target detection, ultrasonic imaging of reverberant multilayer structures, morphological processing and pattern recognition in ultrasonic imaging, time-frequency analysis of ultrasonic signals, and applications of neural networks for detecting target echoes and classifying microstructural scattering. Dr. Saniie has been a technical committee member of the IEEE Ultrasonics Symposium since 1987 (currently he is the chair of Sensors, NDE, and Industrial Applications), Associate Editor of the *IEEE Transactions on Ultrasonics, Ferroelectrics, and Frequency Control* since 1994, IEEE Branch Counselor (1983–1990), Program Coordinator and Local Chair of the Conference on Properties and Applications of Magnetic Materials (1985–2005), and Editorial Advisory member of the *Nondestructive Testing and Evaluation* journal (1986–1996). He is a member of Sigma Xi, IEEE, Tau Beta Pi, and Eta Kappa Nu. He is the 1986 recipient of the Outstanding IEEE Student Counselor Award. He is the recipient of the 2006 Outstanding Faculty Award and 2007 University Excellence in Teaching Award. Dr. Saniie is an IEEE Fellow for his contributions to "Ultrasonic Signal Processing for Detection, Estimation and Imaging."

Erdal Oruklu (S'01–M'05–SM'09) received his B.S. degree in electronics and communication engineering from the Technical University of Istanbul in 1995 and the M.S. degree in electrical engineering from Bogazici University, Istanbul, Turkey, in 1999. He received his Ph.D. degree in computer engineering from the Illinois Institute of Technology, Chicago, IL, in 2005. He is currently an Assistant Professor in the Department of Electrical and Computer Engineering at the Illinois Institute of Technology, where he is also the Director of the VLSI and SoC Research Laboratory. Dr. Oruklu's research interests are reconfigurable computing, advanced computer architectures, hardware/software co-design, and embedded systems. Dr. Oruklu has published more than 100 journal and conference papers on real-time ultrasonic systems and FPGA hardware. He has also co-authored five book chapters. Dr. Oruklu is a member of the IEEE International Ultrasonics Symposium Technical Program Committee, a senior member of IEEE, and a member of Eta Kappa Nu.
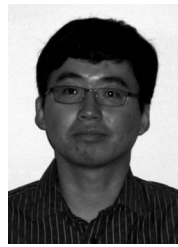
Sungjoon Yoon received his B.S. degree in electronic materials and devices engineering from Inha University of Inchon, South Korea, in 1996. He received his M.S and Ph.D. degrees in electrical engineering from the Illinois Institute of Technology, Chicago, IL, in 2002 and 2010, respectively. He is currently a Hardware Engineer at Honeywell Analytics in Lincolnshire, IL. Dr. Yoon's research interests are digital signal processing and digital system design.